FHWA-1

PILES IN SAND: A DESIGN METHOD INCLUDING RESIDUAL STRESSES

by

Jean-Louis Briaud[1] and Larry Tucker[2]

An article proposed for publication in
the Geotechnical Engineering Journal of
the American Society of Civil Engineers

October 1983

1. Associate Professor, Civil Engineering Department, Texas A&M University, College Station, TX 77843

2. Research Assistant, Civil Engineering Department, Texas A&M University, College Station, TX 77843

Keywords

Piles, Sand, Residual Stresses, Design, Load Test, Vertical Load

Abstract

A design method for piles driven in sand and subjected to static vertical loads is presented. This method is unique in that it considers the existence of residual stresses due to driving. It uses the results of Standard Penetration Tests to obtain the load transfer curves for friction and point resistance. These curves are modelled by hyperbolas which start at the residual friction and residual point pressure for zero displacement.

The design method is based on a simple theory, and on a 33 piles data base. The residual stresses and the transfer curves could be determined with reasonable accuracy from the data base because for each pile there was sufficient instrumentation and the load test program was sufficiently complete.

The Phenomenon of Residual Stresses

During a hammer blow, a pile will move downward first, then rebound and then oscillate around a final position. At its final position the pile is in equilibrium under a certain point load and a certain friction load, which cancel out since the top load is zero. The process repeats itself during the full driving sequence of the pile and when the pile reaches final penetration the load distribution in the pile can be as shown on Fig. 1.

During the downward movement of the pile the pile-soil friction is acting upward on the pile to resist the penetration of the pile; the point soil resistance is also acting upward. During the rebound that follows, the soil under the point pushes the pile back up while the pile decompresses elastically. These two components of the rebound create enough upward movement to reverse the direction of the pile-soil friction which now acts downward at least in the upper portion of the pile. Equilibrium is reached when enough of the friction stresses have reversed themselves in order to keep the bottom of the pile prestressed against the soil.

The above explanation shows that the residual stresses phenomenon is governed by the unloading characteristics of the point and friction transfer curves (q-w and f-w curves) on one hand, and by the elastic characteristics of the pile on the other. In sands, a significant residual point load can exist because point capacities are large and because little movement is needed to unload the friction transfer curve, while much more movement is needed to unload the point transfer curve.

The existence of residual stresses has been known for a long time (7, 6) but has not been routinely included in pile design.

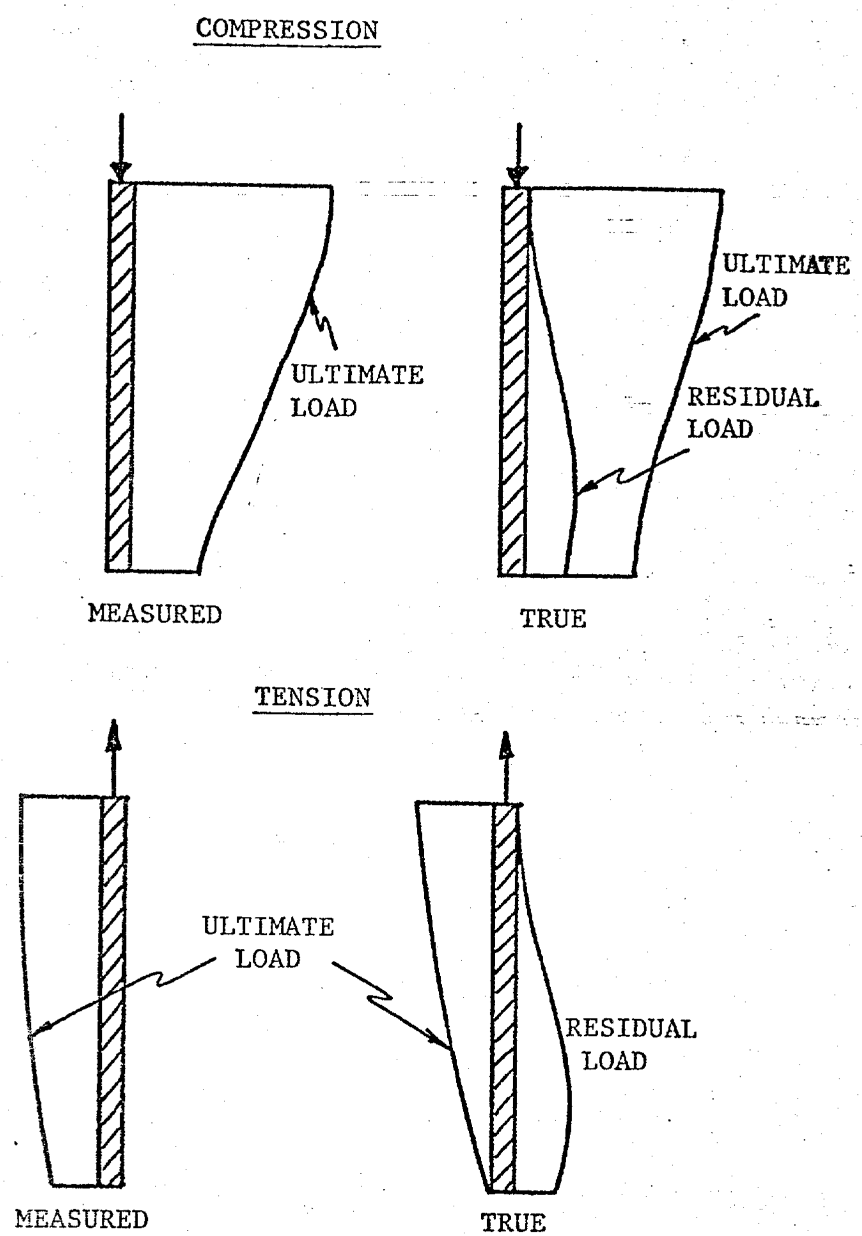

FIG. 1: Load in Piles

Why are Residual Stresses Important?

In a conventional load test on an instrumented pile, the following testing sequence is usually observed: first the pile is instrumented, second the pile is driven, third the instrumentation is zeroed, fourth the load test is performed. Zeroing the instrumentation after having driven the pile is equivalent to assuming that zero stresses exist in the pile after driving. Therefore, in a conventional load test residual stresses are not measured.

The difference in load distribution in the pile between the measured loads as described above and the true loads that exist in the pile is shown on Fig. 1 for a compression test and a tension test. As can be seen, the interpretation of the results from a conventional compression test will lead to a point load which is lower than the true point load and to a friction load which is higher than the true friction load.

The interpretation of the results from a conventional tension test on the other hand, will lead to a point load which is larger than the true point load which is zero, and to a friction load which is smaller than the true friction load. Due to these errors in measurements, all the predictive methods based on these conventional load test results are in error. Therefore, for the purpose of developing a predictive method, residual stresses must be considered.

Theoretical Formulation

The following theoretical formulation makes a number of simplifying assumptions. The results are useful however, because they show theoretically the role of the various influencing factors. The residual loads are loads that are locked in upon unloading after the pile has been brought to the ultimate soil resistance. Therefore, the theoretical analysis takes as an initial condition the stress and load distribution in the pile at failure. The ultimate skin friction is τ_U, and the ultimate point resistance is q_U (Fig. 2). The top ultimate load is Q_{TU} and the point ultimate load is Q_{PU}. The load anywhere in the pile is Q_U.

The unloading of the friction is assumed to obey the linear elastic model (Fig. 2):

$$\Delta\tau = K'_\tau \Delta w \quad \text{(1)}$$

where $\Delta\tau$ is the decrease in pile-soil friction stress at depth z
K'_τ is the unloading stiffness in friction
Δw is the upward movement of the pile upon unloading at depth z.

Similarly the unloading of the point follows:

$$\Delta q = K'_p \Delta w_p \quad \text{(2)}$$

where Δq is the decrease in point resistance
K'_p is the unloading stiffness for the point.
Δw_p is the upward movement of the pile at the point upon unloading.

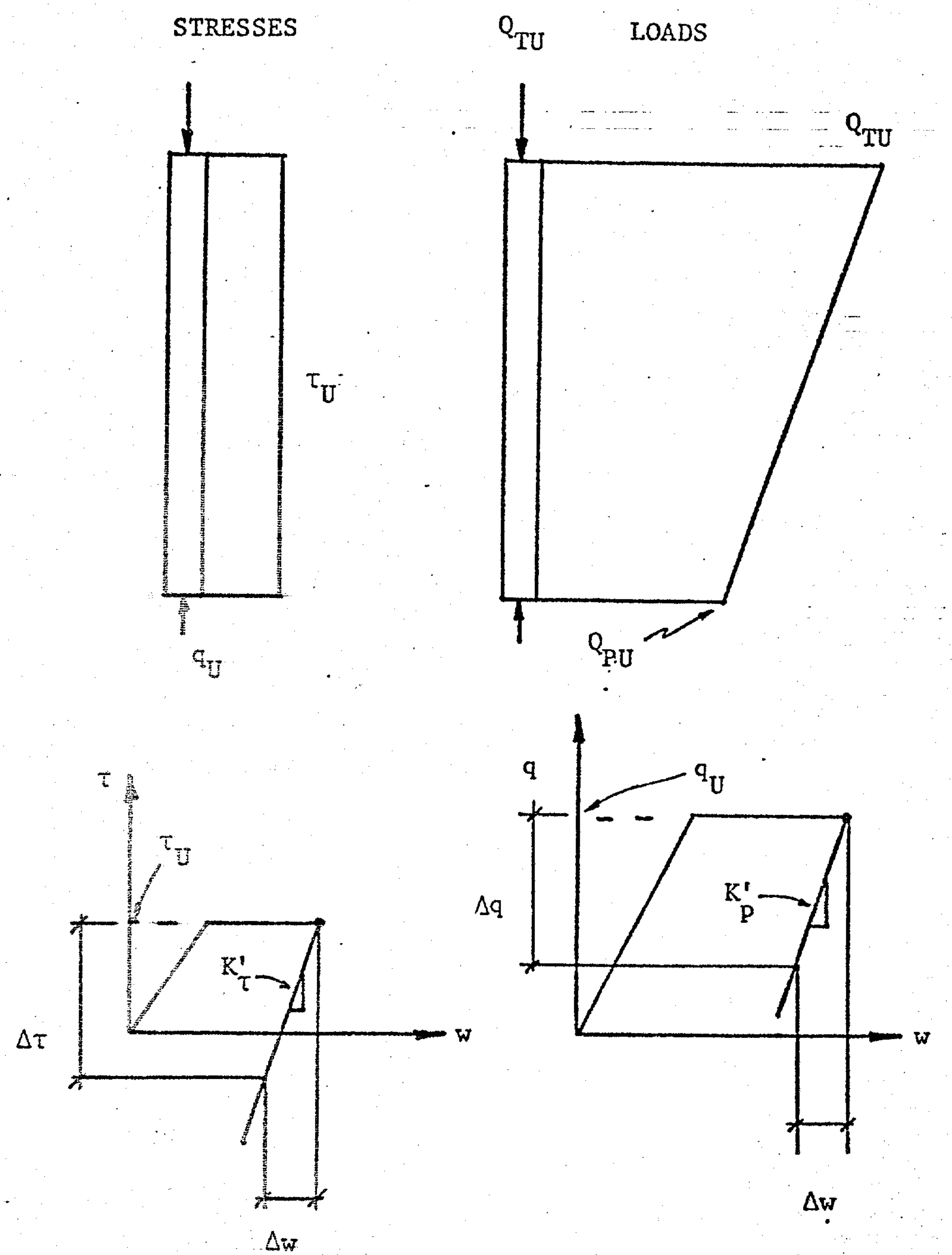

FIG.2 - Unloading Process for Residual Loads

The equilibrium of the elementary pile element can be written incrementally as follows (1):

$$-\frac{\partial \Delta\sigma}{\partial z} - \frac{P}{A}\Delta\tau = 0 \quad \ldots\ldots\ldots\ldots\ldots\ldots \quad (3)$$

where $\Delta\sigma$ = normal stresses decrease in pile at depth z

A = cross sectional area of pile.

P = perimeter of pile.

The constitutive equation for the pile is:

$$\Delta\sigma = E_p\Delta\varepsilon = -E_p\frac{\partial \Delta w}{\partial z} \quad \ldots\ldots\ldots\ldots\ldots\ldots \quad (4)$$

where E_p is the pile modulus

$\Delta\varepsilon$ is the decrease in normal strain at depth z due to unloading.

The solution to the problem gives the residual load (Q_R) in the pile at a depth z (1):

$$Q_R = Q_U - Q_{TU}\left[\frac{(E_p\Omega+K'_p)e^{\Omega(L-z)} - (E_p\Omega-K'_p)e^{-\Omega(L-z)}}{(E_p\Omega+K'_p)e^{\Omega L} - (E_p\Omega-K'_p)e^{-\Omega L}}\right] \quad \ldots \quad (5)$$

where L is the length of the pile

z is the depth at which Q_R exists

and

$$\Omega = \sqrt{\frac{K'_\tau P}{E_p A}}$$

The residual point load, Q_{PR}, is:

$$Q_{PR} = Q_{PU} - \frac{2\ Q_{TU}}{\left[1 + \frac{E_p \Omega}{K'_p}\right] e^{\Omega L} + \left[1 - \frac{E_p \Omega}{K'_p}\right] e^{-\Omega L}} \quad \ldots\ldots\ldots\ldots \quad (6)$$

Equation 5 and 6 show that the factors influencing the distribution and magnitude of residual loads are the ultimate point and total loads, the pile length, the relative pile-soil stiffness.

Data Base

The study was restricted to vertical pile load tests on instrumented piles hammer driven in sand (1). A review of the literature revealed 10 sites with a total of 33 instrumented piles. Details of the piles and soil data available at the sites are presented in Table 1.

The q-w curve is the load transfer curve at the point of the pile. The parameter q is the average pressure under the point for a movement w of the pile point. An f-w curve is a load transfer curve along the shaft of the pile. The parameter f is the friction developed between the soil and the pile for a movement w of the pile shaft. On Figure 3, the dotted curves represent the load transfer curves obtained from conventional load tests where residual stresses are ignored, while the solid lines represent the load transfer curves including residual stresses.

The following parameters were used in the analysis of the data base: q_{max} is the true ultimate point pressure, q_{res} is the residual

TABLE 1. - Data Base

SITE (1)	PILE (2)	PILE TYPE AND MATERIAL (3)	DIMENSIONS: DIAMETER ft (4)	DIMENSIONS: LENGTH ft (5)	DIMENSIONS: AREA in^2 (6)	MODULUS OF ELASTICITY psi x 10^6 (7)	TYPE TEST (8)	REFERENCE (9)
Lock and Dam 4 Arkansas River (1963)	1	Steel Pipe	1.20	53.1	17.12	29.0	C, T	
	2	Steel Pipe	1.50	52.8	23.86	29.0	C, T	
	3	Steel Pipe	1.70	53.0	27.36	29.0	C, T	
	6	Steel "H" HP 14x73	1.34	40.0	25.70	29.0	C	3
	7	Steel "H" HP 14x73	1.34	52.1	29.33	29.0	C, T	8
	9	Steel "H" HP 14x73	1.34	53.2	26.28	29.0	C	
	10	Steel Pipe	1.50	53.1	23.86	29.0	C, T	
	16	Steel Pipe	1.42	52.7	19.62	29.0	C, T	
Low Sill Structure Old River, La. (1956)	1	Steel "H" HP 14x73	1.34	80.5	25.70	29.0	C	9
	2	Steel Pipe	1.75	65.1	27.36	29.0	C, T	
	3[a]	Steel "H" HP 14x73	1.34	70.6	25.70	29.0	C	
	4	Steel Pipe	1.42	66.3	22.65	29.0	C, T	
	5	Steel Pipe	1.42	45.1	22.65	29.0	C, T	
	6	Steel Pipe	1.58	65.2	25.00	29.0	C, T	
Ogeechee River (1969)	H-11	Steel Pipe	1.50	9.9	27.49	30.0	C	14
	H-12	Steel Pipe	1.50	20.1	27.49	30.0	C	15
	H-13	Steel Pipe	1.50	29.1	27.49	30.0	C	
	H-14	Steel Pipe	1.50	39.3	27.49	30.0	C	
	H-15	Steel Pipe	1.50	49.3	27.49	30.0	C	
Lock and Dam 26 Replacement Site (1972)	5IP-I	Steel "H" HP 14x73	1.34	80.1	21.40	29.0	T	4
	5IP-II	Steel "H" HP 14x73	1.34	54.4	21.40	29.0	T	
	3IP-IIIS	Steel "H" HP 14x73	1.34	54.0	21.40	29.0	C, T	

TABLE 1 (Continued)

SITE (1)	PILE (2)	PILE TYPE AND MATERIAL (3)	DIMENSIONS DIAMETER ft (4)	LENGTH ft (5)	AREA in^2 (6)	MODULUS OF ELASTICITY psi x 10^6 (7)	TYPE TEST (8)	REFERENCE (9)
West Seattle Freeway Bridge (1980)	A	Octagonal Concrete	2.05	98.0	477.20	5.56	C	11
	B	Octagonal Concrete	2.05	84.0	477.20	5.56	C	12
Tavenas (1970)	H5	Steel "H" 12 BP 74	1.09	60.0	21.80	35.0	C	13
	J5	Hexagonal Concrete	1.05	60.0	127.00	3.94	C	
Gregersen (1969)	A	Circular Concrete	0.92	26.2	95.45	3.15	C	5
	D/A	Circular Concrete	0.92	52.5	95.45	3.15	C	
	C	Tapered Circular Concrete	Top 0.92 Bot. 0.66	26.2	Varied	3.15	C	
	B/C	Straight Cir. to 26.3 ft. Tapered to bottom Concrete	Top 0.92 Bot. 0.66	52.5	Varied	3.15	C	
Corpus Christi (1971)	Init.	Square Concrete	1.50	33.5	256.00	5.6	C	2
	Final	Square Concrete	1.50	33.5	256.00	5.6	C	
Sellgren (1981)	A-I	Square Concrete	1.00	35.4	113.00	3.15	C	10
	A-II	Square Concrete	1.00	35.4	113.00	3.15	C	
Lock and Dam 26 Ellis Island	M6	Timber	Top 1.10 Bot. 0.92	35.0	Varied	2.0	C	16 17

[a]Had a 3/4 in. (1.9 cm) thick square plate on the bottom.

NOTE: 1 ft = 0.305 m; 1 psi = 6.89 kN/m^2

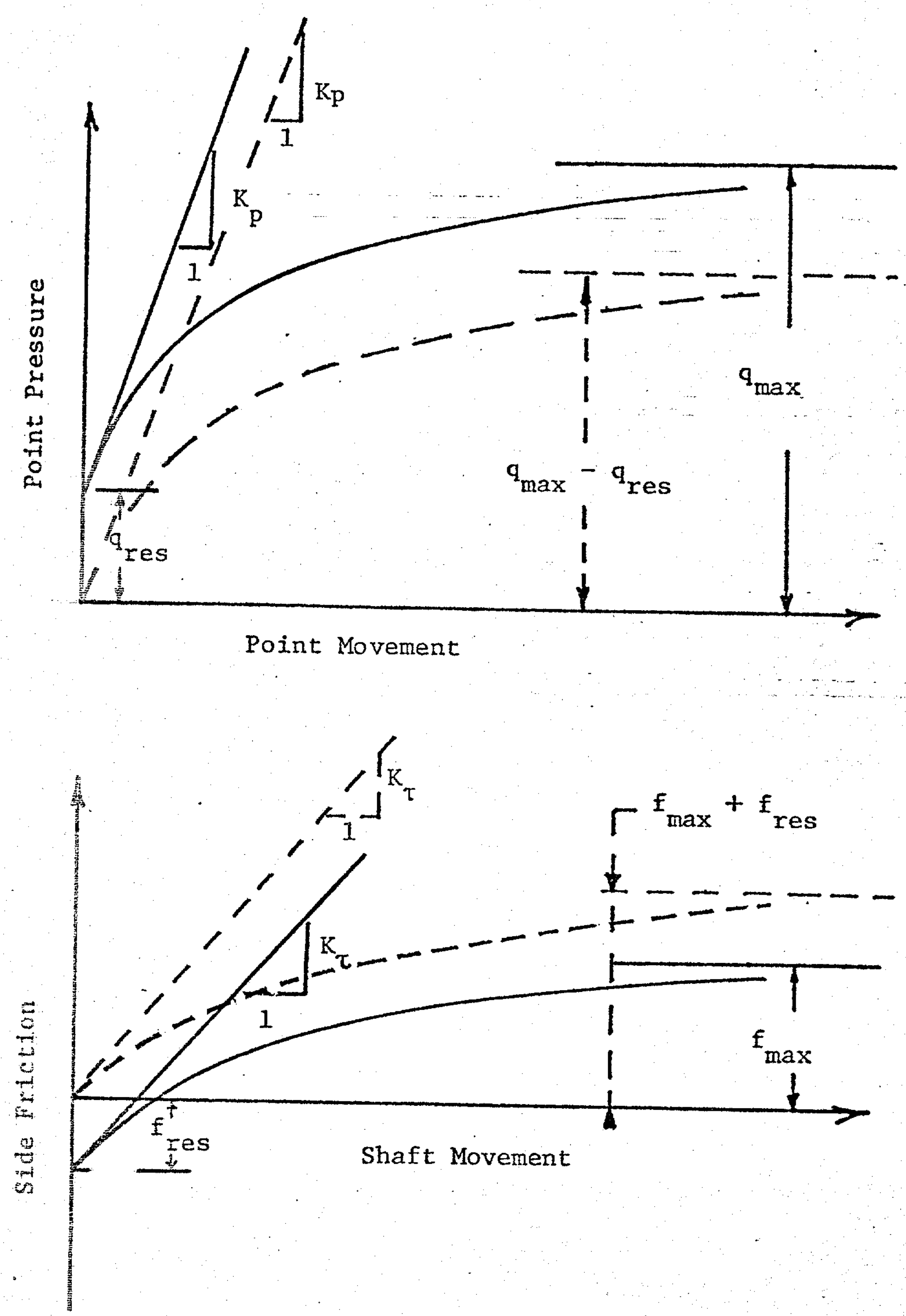

FIG. 3 .- Examples of Hyperbolic Load Transfer Curves

point pressure after driving, f_{max} is the true ultimate friction, f_{res} is the residual friction after driving, K_p is the initial slope of the q-w curve and K_τ is the initial slope of the f-w curve.

The load transfer analysis on these instrumented piles was performed as follows:

1. The f-w and q-w curves were obtained point by point from the load tests without correction for residual stresses.

2. A hyperbolic model was fit through the experimental points of the f-w and q-w curves. This led to curves such as the one shown in dotted line on Figure 3.

3. The equation of the hyperbolas gave K_τ, K_p, $f_{max}-f_{res}$, $q_{max}-q_{res}$ (Fig. 3).

4. The value of the residual point pressure after driving q_{res} and of the residual friction f_{res} were obtained from the load test data by one of four methods (1), depending on the data available. Method 1 consists of reading the pile instrumentation before and after driving. Method 2 is the Hunter-Davisson method (7). Method 3 consists of assuming that in a tension test the load that appears as a tension load on the point is the residual point load. Method 4 consists of assuming that the tension load in a tension test is the true friction load in a compression test.

5. The value of q_{max} and q_{max} were obtained by adding q_{res} and subtracting f_{res} respectively to the values obtained in step 3.

Correlations

A parametric analysis of Equation 6 showed that the parameter ΩL is a a controlling factor in the magnitude of residual point loads. This is why a correlation between q_{res} and ΩL was attempted (Figure 4).

Due to a lack of other soil data at the sites only the SPT results were used in correlations with all other parameters. A decision was made not to use any correction on the blow count N values because various corrections exist and none are widely accepted. The value of N used for the pile point parameters, N_{pt}, is an average over a distance of four diameters either side of the pile point. The value of N used for the friction parameters N_{side} is a weighted average along the length of shaft considered.

The results of all correlations using the least square regression equations are shown on Figures 5 to 8. Part of the drastic scatter which exists in Figures 5 to 8 is due to measurement errors including those associated with the Standard Penetration Test and with the pile load tests.

If the data points of figure 5 were plotted on a natural scale, they would show that q_{max} does not increase linearly with N. With q_{max} in tsf, the ratio q_{max}/N is about 10 for very low N values, becomes about 4 for N values between 10 and 15, and decreases to 1.6 for N equal 50. This nonlinearity can be explained as folows. In very loose sand the SPT blow count is very low, the SPT does not apply a sufficiently large number of blows to densify the sand and the blow count is representative of the sand in its undisturbed state. In very loose sands, however, the pile will apply a large number of blows to the sand, densify it and q_{max} will be much larger than the q_{max} for the undisturbed loose sand. As a result the ratio q_{max}/N is very high. In very

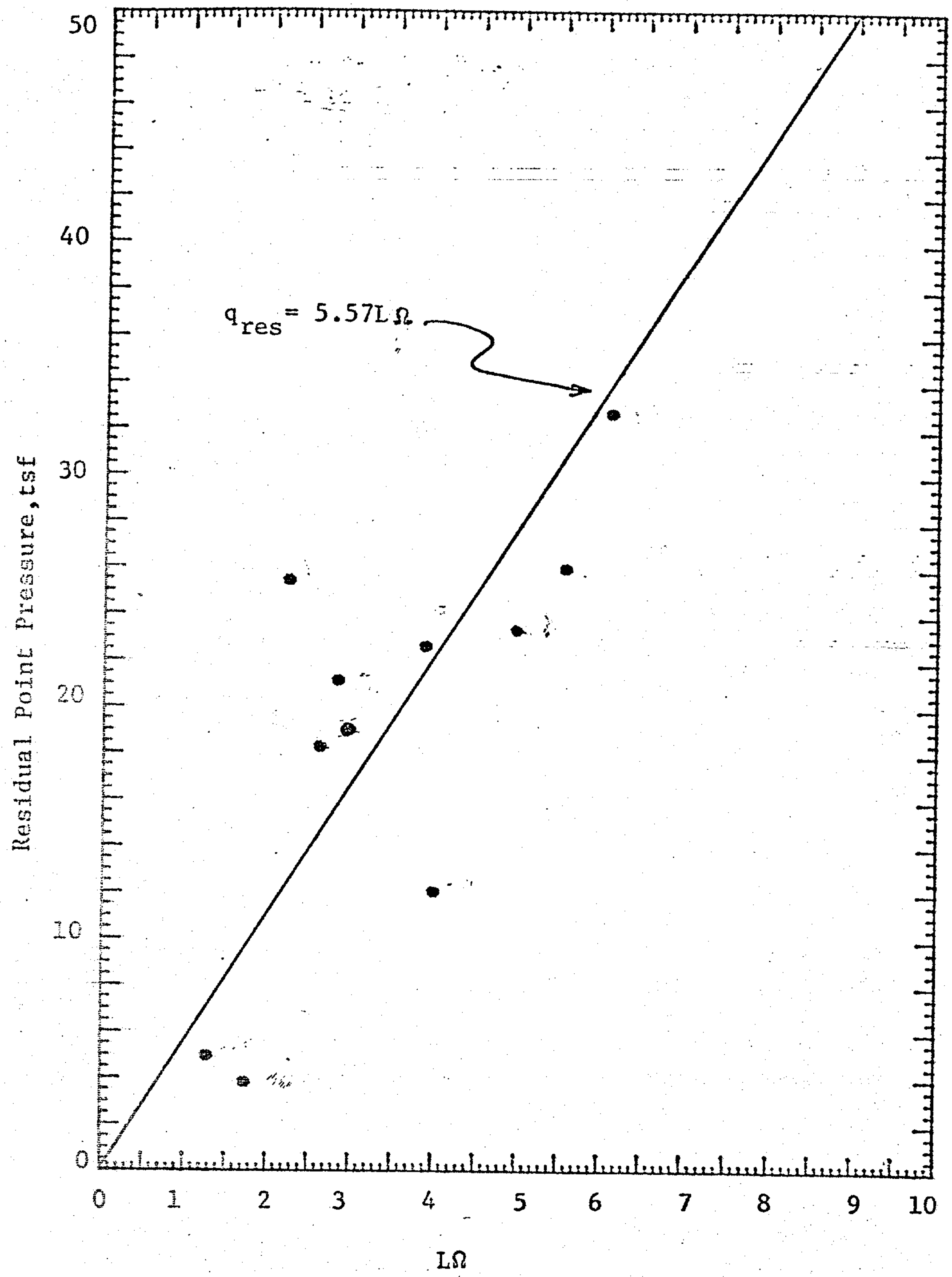

FIG. 4 .- Residual Point Pressure Versus L Ω
(1 tsf = 95.8 kPa)

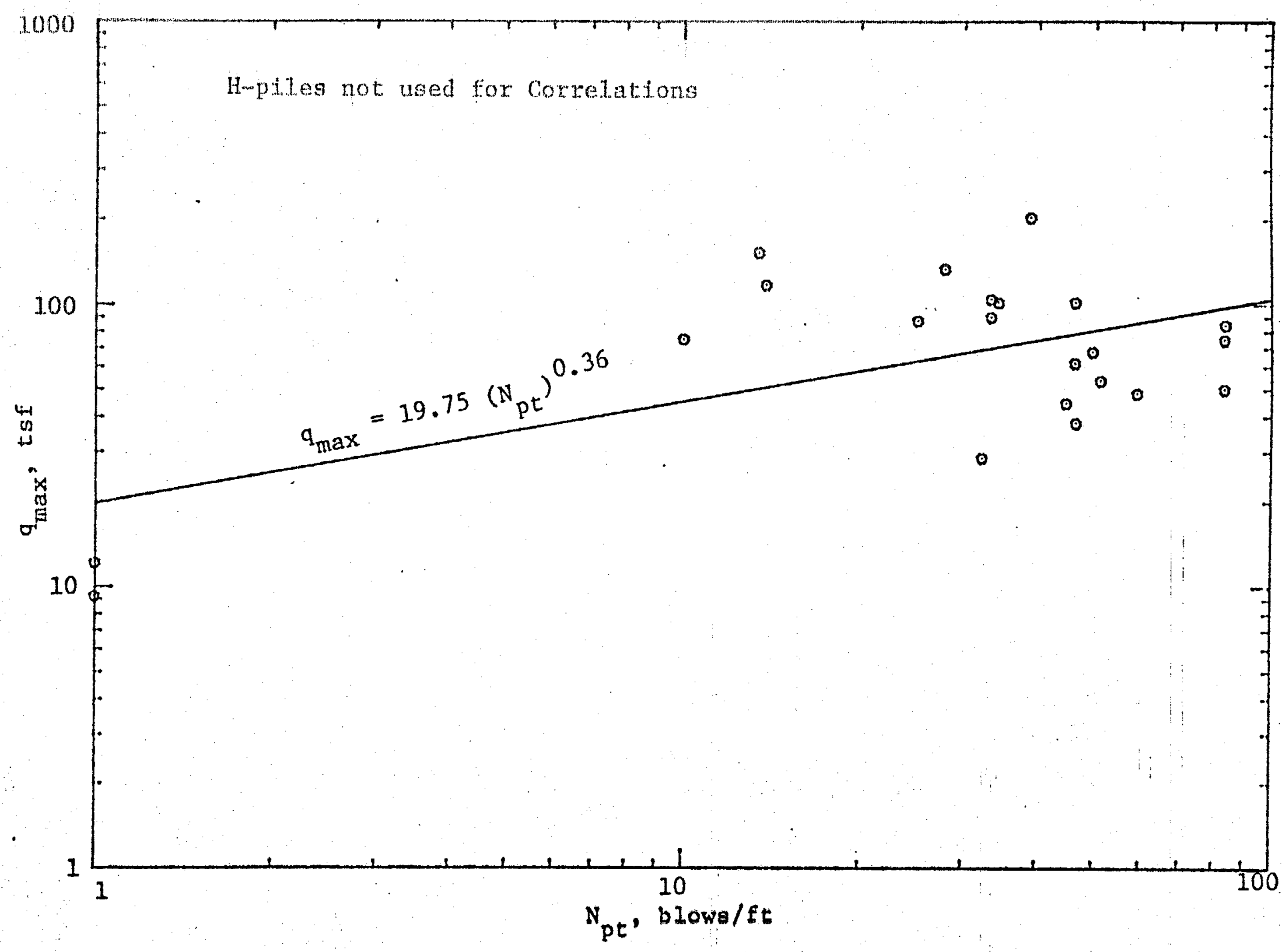

FIG. 5:.- Log (q_{max}) Versus Log (N_{pt}) (1 tsf = 95.8 kPa; 1 blow/ft = 3.28 blow/m)

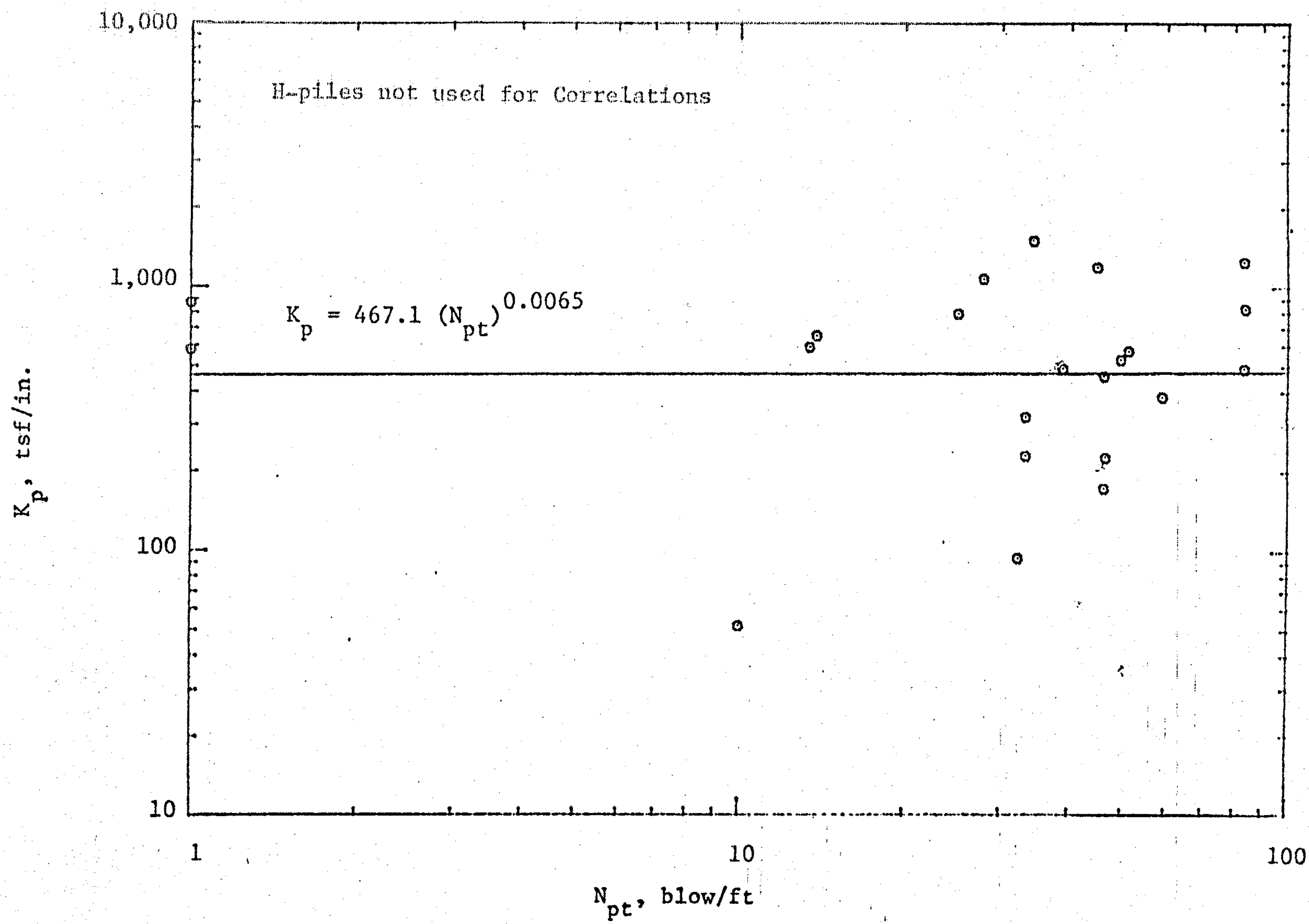

FIG. 6: - Log (K_p) Versus Log (N_{pt})
(1 tsf/in = 37.7 kPa/cm; 1 blow/ft = 3.28 blow/m)

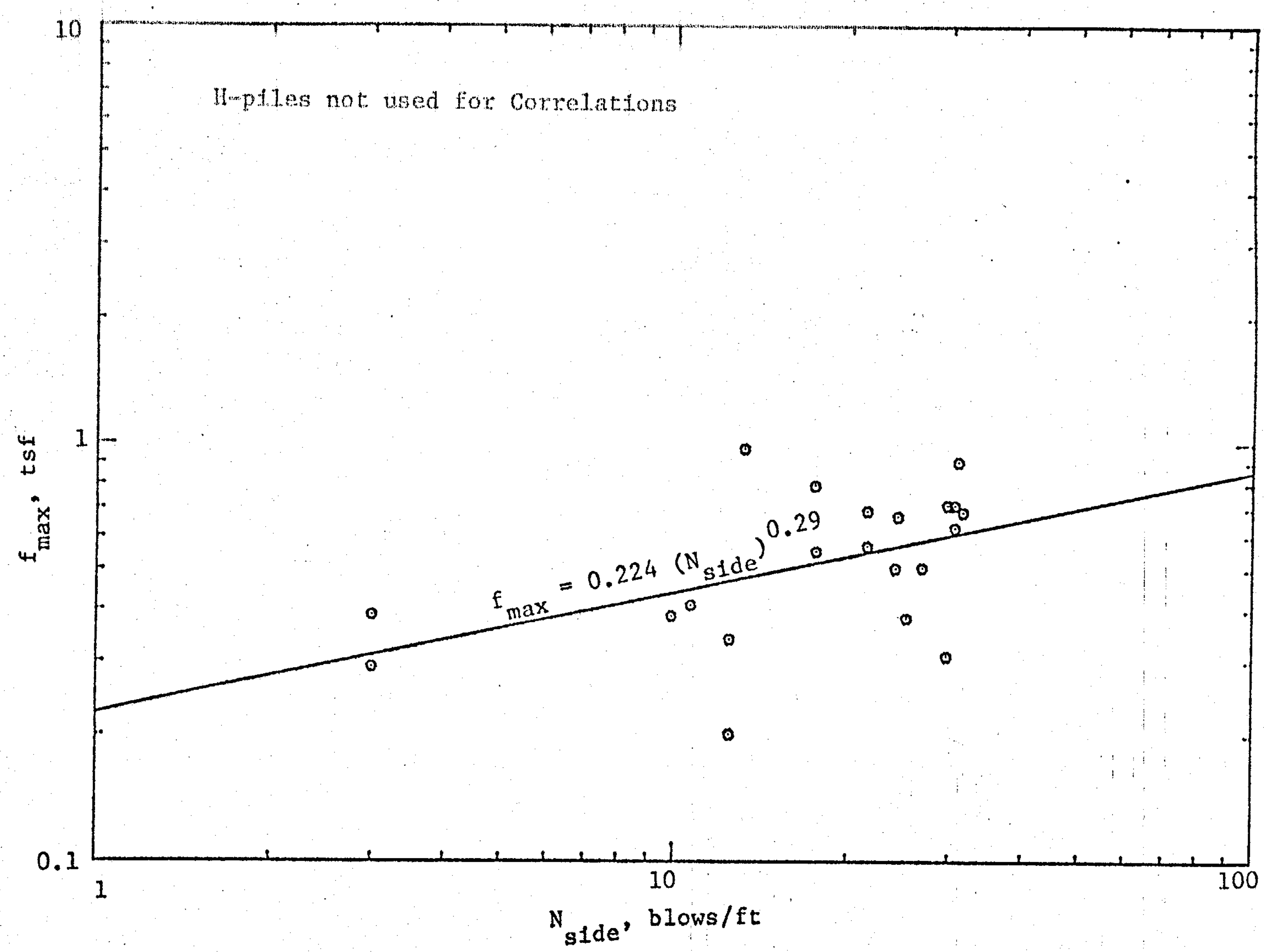

FIG. 7:.- Log (f_{max}) Versus Log (N_{side}) (1 tsf = 95.8 kPa; 1 blow/ft = 3.28 blow/m)

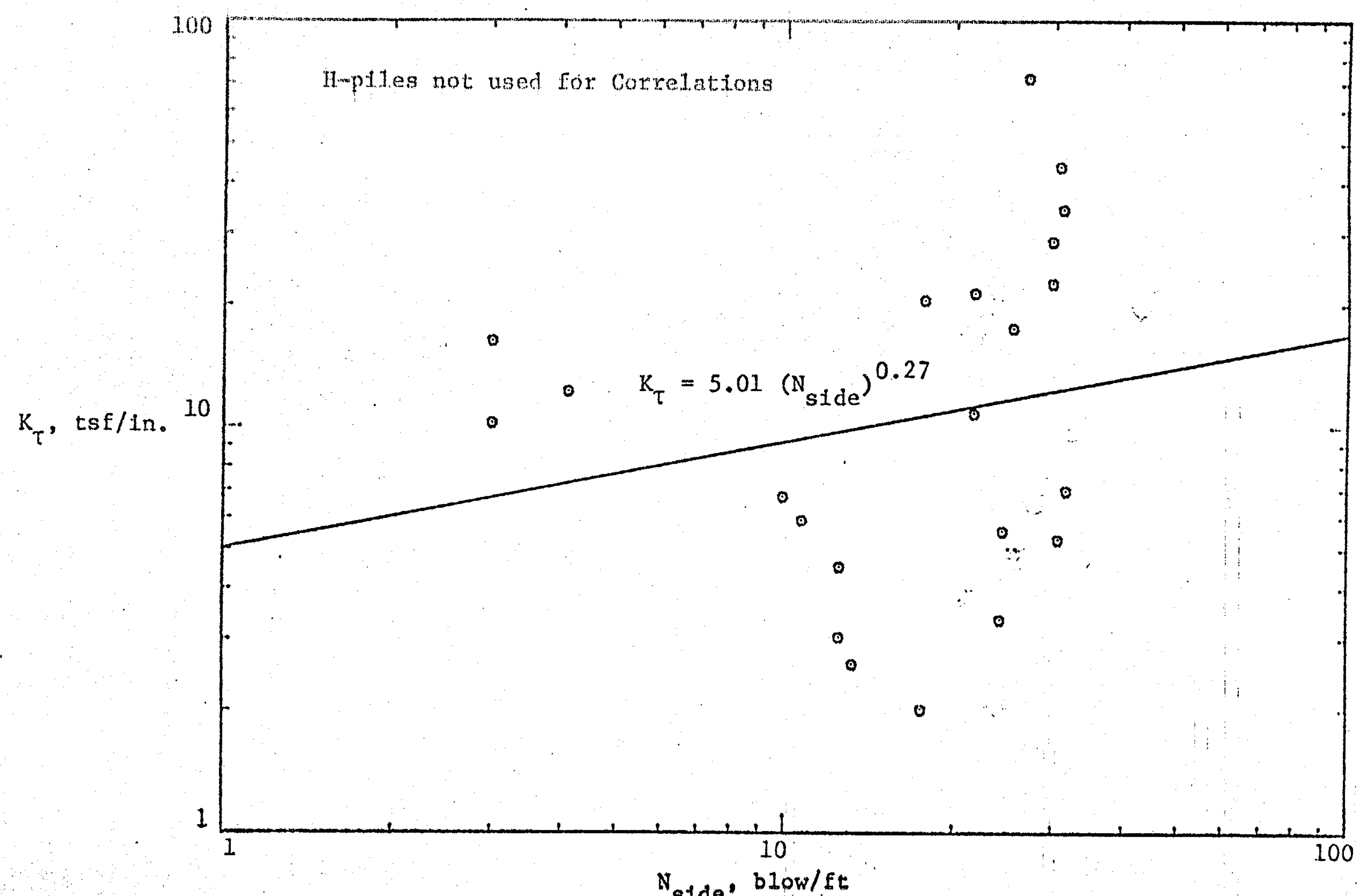

FIG. 8:- Log (K) Versus (N_{side})
(1 tsf/in = 37.7 kPa/cm; 1 blow/ft = 3.28 blow/m)

dense sand, the number of blows for both the SPT and the pile are large and similar soil conditions are created around the split spoon and the pile. As a result the ratio q_{max}/N is much lower than for loose sands.

The Design Method

The f-w and q-w curves for this method do not go through the origin but are offset by an amount equal to the residual stresses after driving (Fig. 3). Both curves are modelled by hyperbolas expressed as (1):

$$q = \frac{w}{\frac{1}{K_p} + \frac{w}{q_{max} - q_{res}}} + q_{res} \quad \ldots\ldots\ldots\ldots\ldots\ldots (7)$$

$$f = \frac{w}{\frac{1}{K_T} + \frac{w}{f_{max} + f_{res}}} - f_{res} \quad \ldots\ldots\ldots\ldots\ldots\ldots (8)$$

in which from the correlations:

$$K_p = 467.1\ (N_{pt})^{0.0065} \quad \ldots\ldots\ldots\ldots\ldots\ldots (9)$$

K_p in tsf/in.

N_{pt} uncorrected average SPT blow count over a distance of four diameters either side of the pile point

$$q_{max} = 19.75\ (N_{pt})^{0.36} \quad \ldots\ldots\ldots\ldots\ldots\ldots (10)$$

q_{max} in tsf

$$q_{res} = 5.57\ L\Omega \quad \ldots\ldots\ldots\ldots\ldots\ldots (11)$$

q_{res} in tsf

L is the pile length

$$\Omega = \sqrt{\frac{K_\tau P}{AE_p}} \quad \text{. . . . .} \quad (12)$$

P = perimeter of the pile

E_p = modulus of the pile

A = cross-section area of the pile

$$K_\tau = 5.01\ (N_{side})^{0.27} \quad \text{. . . . .} \quad (13)$$

K_τ in tsf/in.

N_{side} uncorrected average blow count within shaft length considered.

$f_{max} = 0.224\ (N_{side})^{0.29}$

f_{max} in tsf

$f_{res} = q_{res} \frac{A_p}{A_s}$, and $f_{res} < f_{max}$

In order to predict the load-settlement curve for a pile, an axially loaded pile computer program may be used. Minor modifications must be made to incorporate residual stresses. At zero movement the pile is under a compressive load due to the residual stresses. The elastic compression of the pile under this compressive residual load must be subtracted from all settlements computed by the program. This elastic compression is calculated by using the residual state of stress.

Accuracy of Predictions

The above method was used to generate the load-settlement curves for the piles of the data base (Fig. 9). Figures 10 and 11 are frequency

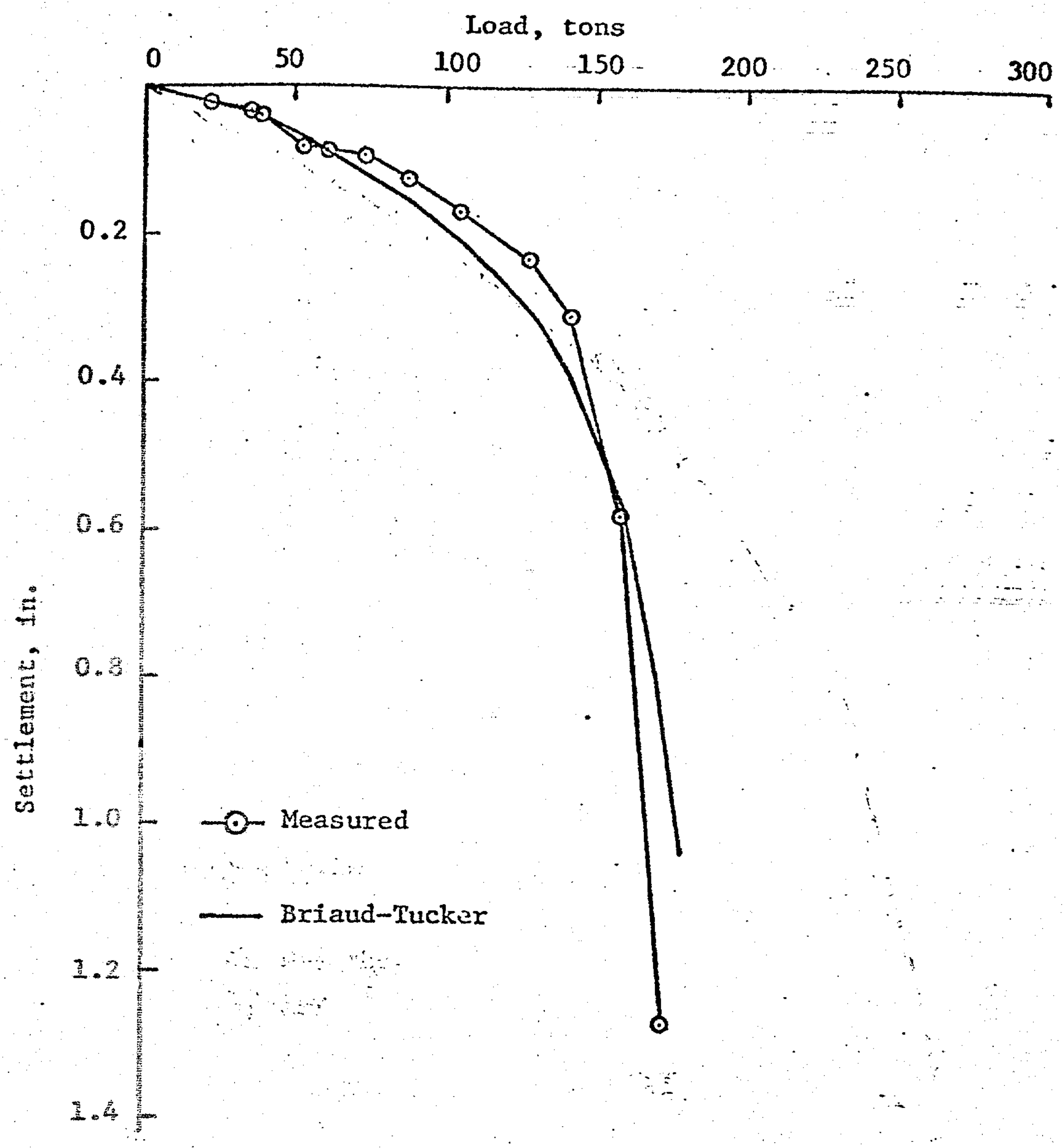

FIG. 9 .- Arkansas River Pile 1: Load-Settlement Predictions by Coyle and Briaud-Tucker Methods (1 ton = 9.058 kN; 1 in. = 2.54 cm)

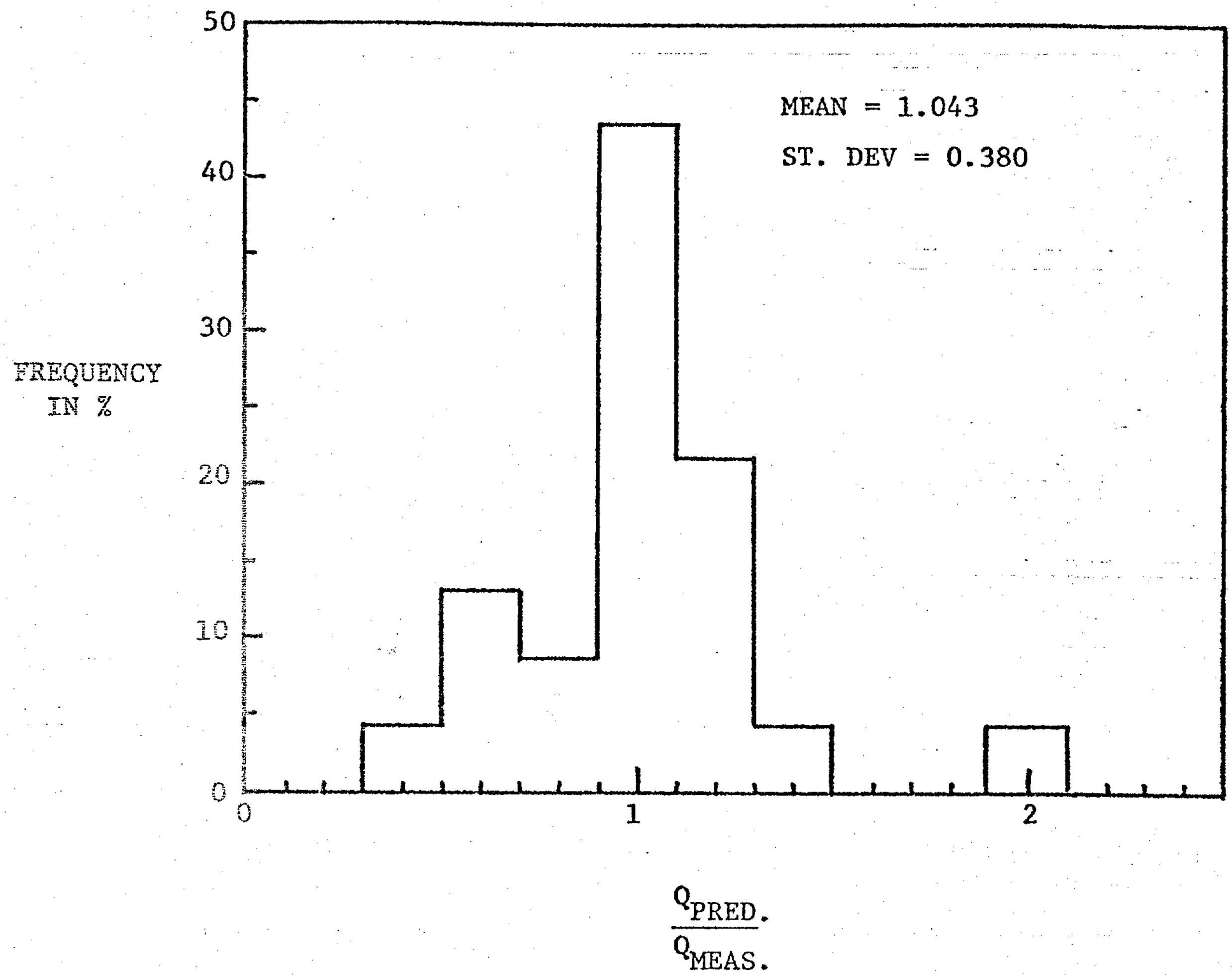

FIG. 10: Frequency Distribution for Ultimate Capacity

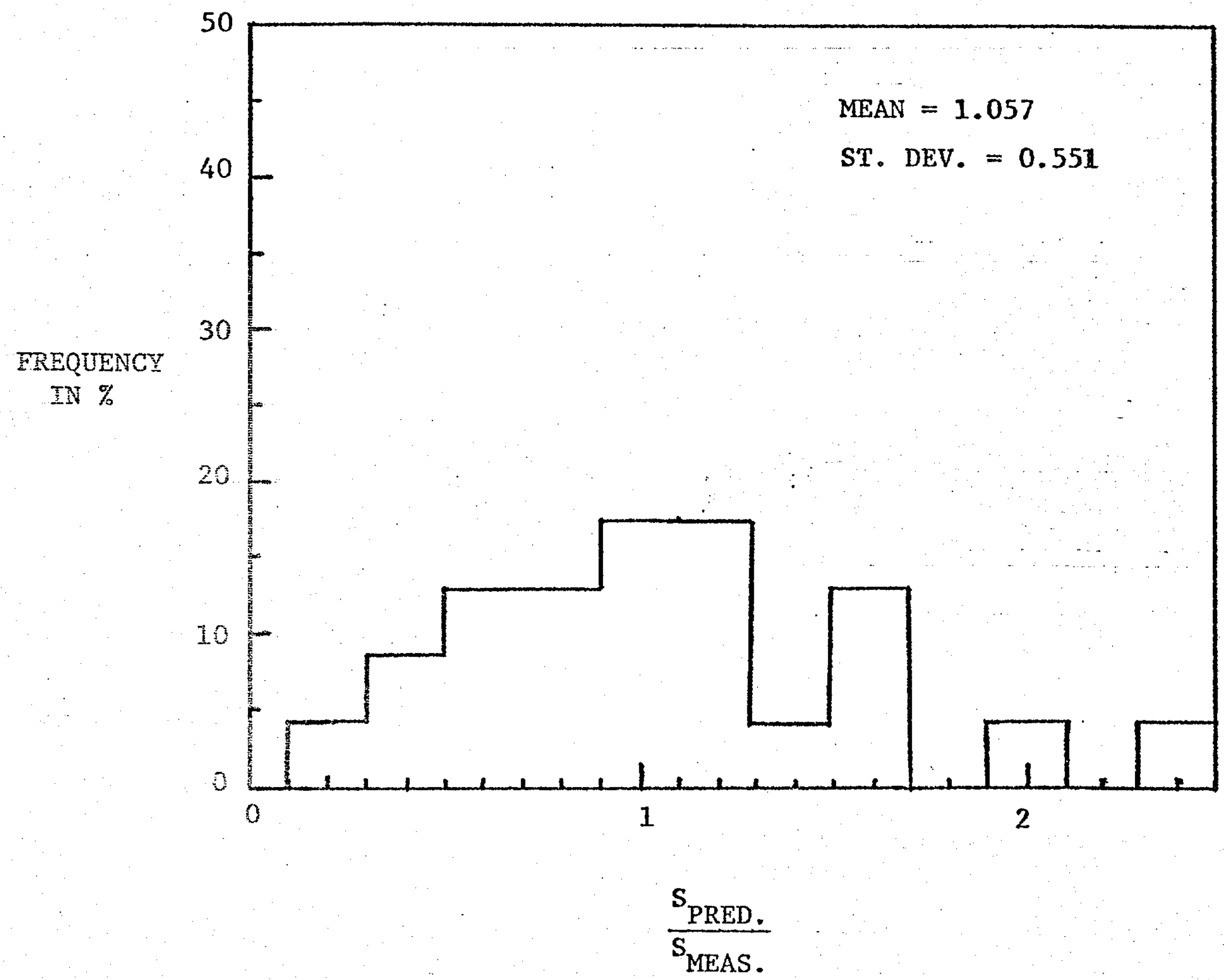

FIG. 11: Frequency Distribution for Settlement

distributions which give an idea of the precision of the method. On Fig. 10, Q_{meas} is the load measured during the load test at a settlement equal to 10% of the pile diameter, while Q_{pred} is the load predicted at the same settlement. On Fig. 11, S_{meas} is the settlement measured at a load equal to 1/2 Q_{meas} and S_{pred} is the settlement predicted at the same load. These figures do not give a true idea of accuracy since they show the precision of the method on the data base used to develop it.

The limitations of the method are tied to the data base; this data base included driven piles that averaged 50 ft in length and 1.3 ft in diameter. The sands varied from very fine to very coarse and from loose to very dense.

Conclusion

A method is presented for the design of hammer driven piles in sand. This method is different from most previously available methods in that it includes the consideration of residual driving stresses. Based on a 33 piles data base, and on the results of Standard Penetration Tests, hyperbolic models are used to describe the friction and point pressure transfer curves. The method therefore allows to predict the entire top load top-movement curve for the pile.

Acknowledgements

The results presented in this article are part of a study performed for the Federal Highway Administration and the United States Geological Survey under Contract No. DTFH 61-82-C-0038. The contact persons were

Carl Ealy and Charles Smith. The team of researchers included H.M. Coyle, R.A. Hawkins, L.L. Lowery, R.L. Lytton, M.W. O'Neill.

REFERENCES

1. Briaud, J.-L., Tucker, L.M., Lytton, R.L., Coyle, H.M., "The Behavior of Piles and Pile Groups in Cohesionless Soils," Federal Highway Administration Report No. RD-83-38, October 1983.

2. Coyle, H.M., Bartoskewitz, R.E., and Berger, W.J., "Bearing Capacity Prediction by Wave Equation Analysis - State of the Art," Research Report No. 125-8, Texas Transportation Institute, Texas A&M University, August, 1973.

3. Fruco and Associates, "Pile Driving and Loading Tests," Report for Corps of Engineers, Little Rock, Arkansas, September, 1964.

4. Fruco and Associates, "Overwater Steel H-pile Driving and Testing Program," Report for Corps of Engineers, St. Louis, Missouri, September, 1973.

5. Gregersen, O.S., Aas, G., and DiBiaggio, E., "Load Tests on Friction Piles in Loose Sand," Proceedings of the VII International Conference on Soil Mechanics and Foundation Engineering, Moscow, Vol. 2.1, 1973, pp. 19-27.

6. Holloway, D.M., Clough, G.W., and Vesic, A.S., "The Mechanics of Pile-Soil Interaction in Cohesionless Soils," Report for Corps of Engineers, Vicksburg, Miss., Dec., 1975.

7. Hunter, A.H., and Davisson, M.T., "Measurements of Pile Load Transfer," Performance of Deep Foundations, ASTM STP 444, 1969, pp. 106-117.

8. Mansur, C.I., and Hunter, A.H., "Pile Tests - Arkansas River Project," Journal of the Soil Mechanics and Foundation Division, ASCE, Vol. 96, No. SM5, September, 1970, pp. 1545-1582.

9. Mansur, C.E., and Kaufman, R.I., "Pile Tests, Low-Sill Structure, Old River, Louisiana," Transactions of ASCE, Vol. 123, 1958, pp. 715-748.

10. Sellgren, E., "Friction Piles in Non-Cohesive Soils, Evluation from Pressuremeter Tests," Thesis, Chalmers University of Technology, Goteborg, Sweden, 1982.

11. Shannon & Wilson, Inc., "Geotechnical Engineering Studies: West Seattle Freeway Bridge Replacement," Report for Anderson-Bjornstad-Kane-Jacobs, Inc., Vol. 2, August, 1980.

12. Shannon & Wilson, Inc., "Instrumentation Installation and Initial Monitoring Pier EA-31," Report for City of Seattle, FHWA (Progress Report 1), November, 1982.

REFERENCES (Con't)

13. Tavenas, F.A., "Load Tests on Friction Piles in Sand," Canadian Geotechnical Journal, Vol. 8, No. 7, 1971, pp. 7-22.

14. Vesic, A.S., "A Study of Bearing Capacity of Deep Foundations," Project B-189, (Final Report), Georgia Institute of Technology, August, 1966.

15. Vesic, A.S., "Tests on Instrumented Piles, Ogeechee River Site," Journal of the Soil Mechanics and Foundation Divisions, ASCE, Vol. 96, No. SM2, March, 1970, pp. 561-583.

16. Woodward-Clyde Consultants, "Results and Interpretation of Pile Driving Effects Test Program," Phase IV Report for Corps of Engineers, Vol. III, St. Louis, Missouri, July, 1979.

17. Woodward-Clyde Consultants, "Axial Load Tests Monoliths M5 and M6," Supplemental Report to Corps of Engineers, St. Louis, Missouri, February, 1980.